CLE-CLAVATA1 peptide-receptor signaling module regulates the expansion of plant root systems in a nitrogen-dependent manner

Takao Araya[a,b,c], Mayu Miyamoto[b], Juliarni Wibowo[b], Akinori Suzuki[b], Soichi Kojima[b,1], Yumiko N. Tsuchiya[b], Shinichiro Sawa[d,2], Hiroo Fukuda[d], Nicolaus von Wirén[c], and Hideki Takahashi[a,b,e,3]

[a]Department of Biochemistry and Molecular Biology, Michigan State University, East Lansing, MI 48824; [b]RIKEN Plant Science Center, Yokohama 230-0045, Japan; [c]Molecular Plant Nutrition, Leibniz Institute of Plant Genetics and Crop Plant Research, D-06466 Gatersleben, Germany; [d]Department of Biological Sciences, Graduate School of Science, University of Tokyo, Tokyo 113-0033, Japan; and [e]Kihara Institute for Biological Research, Yokohama City University, Yokohama 244-0813, Japan

Edited by Philip N. Benfey, Duke University, Durham, NC, and approved December 16, 2013 (received for review October 22, 2013)

Morphological plasticity of root systems is critically important for plant survival because it allows plants to optimize their capacity to take up water and nutrients from the soil environment. Here we show that a signaling module composed of nitrogen (N)-responsive CLE (CLAVATA3/ESR-related) peptides and the CLAVATA1 (CLV1) leucine-rich repeat receptor-like kinase is expressed in the root vasculature in *Arabidopsis thaliana* and plays a crucial role in regulating the expansion of the root system under N-deficient conditions. *CLE1*, *-3*, *-4*, and *-7* were induced by N deficiency in roots, predominantly expressed in root pericycle cells, and their overexpression repressed the growth of lateral root primordia and their emergence from the primary root. In contrast, *clv1* mutants showed progressive outgrowth of lateral root primordia into lateral roots under N-deficient conditions. The *clv1* phenotype was reverted by introducing a *CLV1* promoter-driven *CLV1:GFP* construct producing CLV1:GFP fusion proteins in phloem companion cells of roots. The overaccumulation of *CLE2*, *-3*, *-4*, and *-7* in *clv1* mutants suggested the amplitude of the CLE peptide signals being feedback-regulated by CLV1. When *CLE3* was overexpressed under its own promoter in wild-type plants, the length of lateral roots was negatively correlated with increasing *CLE3* mRNA levels; however, this inhibitory action of CLE3 was abrogated in the *clv1* mutant background. Our findings identify the N-responsive CLE-CLV1 signaling module as an essential mechanism restrictively controlling the expansion of the lateral root system in N-deficient environments.

root morphology | root system architecture | nitrogen signaling

Living organisms have developed dynamic strategies to explore nutrients in the environment. Morphological plasticity of plant roots and microorganisms is often compared with foraging behavior of animals. Plant roots are highly dynamic systems because they can modify their structure to reach nutrient resources in soil and optimize their nutrient uptake capacities. This strategy appears to be associated with morphological adaptation, because plants are sessile in nature and nutrient availabilities in soil are often altered by surrounding biotic and abiotic factors and climate changes. Morphological modifications of plant root systems are particularly prominent when they grow in soil environments with unbalanced nutrient availabilities (1–4). Among the essential elements required for plant growth, nitrogen (N) has a particularly strong effect on root development (1–6). Lateral roots can be developed in N-rich soil patches where adequate amounts of nitrate (NO_3^-) or ammonium (NH_4^+) are available, whereas this local outgrowth of lateral roots is restricted in N-deficient patches (7–9). In addition to these local N responses, lateral root growth is stimulated in response to mild N deficiency and suppressed under excess N supply by systemic plant signals carrying information on the nutritional status of distant plant organs (4, 10–13). These morphological responses are important for plant fitness and N acquisition, despite the cost for structuring the root system architecture (2, 6). However, lateral root growth is not sustained when plants are deprived of N for an extended period (4). Under such severe circumstances, the development of new lateral roots should rather be restricted to prevent the risk of extending roots into N-poor environments. Economizing the cost for root development appears to be an important morphological strategy for plant survival.

To modify root traits in response to changing N availabilities, plants use various types of signaling molecules including hormones and small RNAs (10, 13–17). In particular, auxin signaling proteins and auxin transporters have been proven essential for lateral root development in response to local nitrate supplies (10, 14–17). These proteins are involved in increasing auxin sensitivity or auxin accumulation at lateral root initials or lateral root tips exposed to NO_3^-, and the NRT1.1 nitrate transporter has been suggested to play a key role in NO_3^- sensing (8, 17, 18). In addition, mutations of the nitrate transporter NRT2.1 have been shown to repress or stimulate lateral root initiation depending on N conditions and sucrose supply (12, 19). Thus, N-dependent root development is apparently under control of complex mechanisms, although its signaling components have remained largely unidentified. In this study, we have identified several homologs of the CLE (CLAVATA3/ESR-related) gene family (20–24) to be up-regulated by N deficiency and involved in this yet unresolved regulatory mechanism. CLAVATA3 (CLV3) is known as a signaling peptide that binds to the CLAVATA1 (CLV1)

Significance

Morphological adjustment is an important strategy for survival of living organisms in challenging environments. Plasticity of the root system architecture is critical for nutrient acquisition in plants. Among the essential elements, nitrogen (N) strongly affects root development. This article uncovers a key signaling mechanism regulating the outgrowth of lateral roots and expansion of plant root systems. The mechanism demonstrated in this study suggests an important morphological strategy for plant survival in N-poor environments.

Author contributions: T.A. and H.T. designed research; T.A., M.M., J.W., A.S., S.K., and Y.N.T. performed research; T.A., M.M., S.S., H.F., N.v.W., and H.T. analyzed data; and T.A., N.v.W., and H.T. wrote the paper.

The authors declare no conflict of interest.

This article is a PNAS Direct Submission.

[1]Present address: Department of Applied Plant Science, Graduate School of Agricultural Science, Tohoku University, Sendai 981-8555, Japan.

[2]Present address: Department of Biological Science, Graduate School of Science and Technology, Kumamoto University, Kumamoto 860-8555, Japan.

[3]To whom correspondence should be addressed. E-mail: htakaha@msu.edu.

This article contains supporting information online at www.pnas.org/lookup/suppl/doi:10.1073/pnas.1319953111/-/DCSupplemental.

leucine-rich repeat receptor-like kinase (LRR-RLK) and controls stem cell differentiation in the shoot apical meristem (25–32). CLE-receptor signaling modules are also known to control meristem function in the primary and lateral roots (33–35). The N-responsive CLE peptides described in the present study belong to the group of CLE peptides with the highest sequence similarity to CLAVATA3 (CLV3) (21–23) and may partly substitute for CLV3 in the shoot apical meristem (31, 36, 37). Our present findings indicate that the N-responsive CLE peptides and CLV1 are signaling components required for translating an N-deficient nutritional status into a morphological response inhibiting the outgrowth of lateral root primordia in *Arabidopsis*. The present study demonstrates a unique function of the CLE-CLV1 signaling module in roots and provides new insights into signaling mechanisms regulating the expansion of the plant root system in N-deficient environments.

Results

***CLE* Gene Expression Is Altered in Roots Under N-Deficiency.** To investigate the N responses of CLE peptides and their involvement in root development, we conducted a gene-expression survey of *CLE* gene family members in *Arabidopsis* transcriptome data. Datasets of N-starved roots (13), N-starved and N-supplied young seedlings (38), and N-resupplied roots (16, 39–41) were analyzed. In this initial survey, *CLE3* was found to be induced by N deprivation (Fig. S1 *A* and *B*). *CLE2*, *CLE3*, and *CLE6* were also found to show positive responses to resupply of N (Fig. S1 *B–F*). Based on these observations, we conducted real-time PCR analysis of *CLE1*, *-2*, *-3*, *-4*, *-5*, and *-7* in roots of 14-d-old wild-type *Arabidopsis* seedlings grown with various NO_3^- supplies. A detailed analysis of *CLE6* was not conducted because *CLE6* mRNA was not detectable in roots under our experimental conditions. In this experiment, we found a significantly higher accumulation of *CLE1*, *-3*, *-4*, and *-7* transcripts under N-deficient conditions (<100 μM NO_3^-) (Fig. 1*A*).

Overexpression of CLE Peptides Inhibits Lateral Root Development. To investigate the roles of N deficiency-responsive CLE peptides and their homologs in root development, *CLE1*, *-2*, *-3*, *4*, *-5*, and *-7* were constitutively overexpressed under control of the cauliflower mosaic virus 35S promoter (Fig. 1 *B–D* and Fig S1 *G–J*), which led to high expression levels of *CLE* genes in these transgenic lines (Fig. S1*G*). In agreement with a previous study (36), the overexpressors for *CLE1*, *-2*, *-3*, *-4*, *-5*, and *-7* showed a delay in flowering (Fig. S2*A*). A subsequent analysis of root phenotypes showed that primary root growth was not affected but total lateral root length was significantly shorter in any of

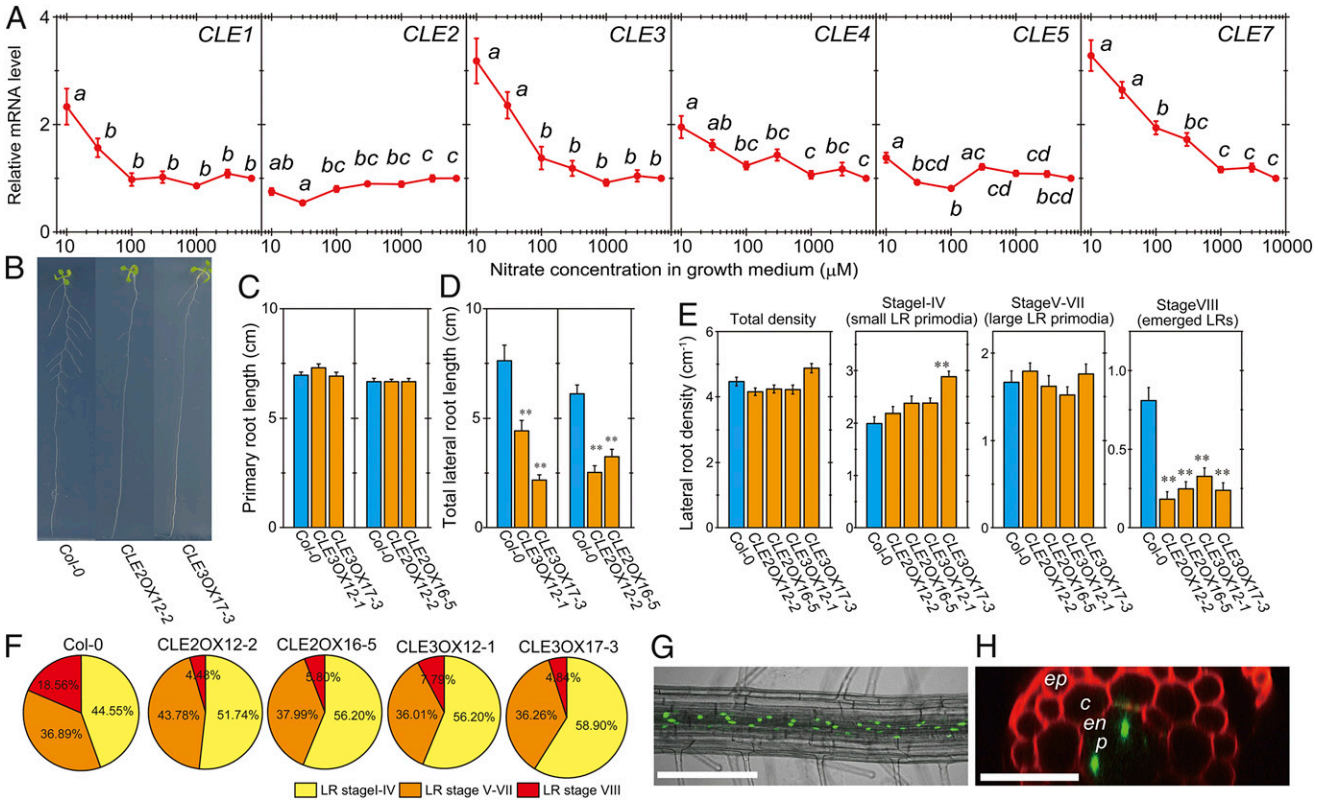

Fig. 1. Constitutive overexpression of *CLE2* and *CLE3* represses lateral root development. (*A*) Regulation of *CLE1* to *7* transcript levels by nitrogen supply. Wild-type (Col-0) plants were grown for 14 d on medium with various NO_3^- concentrations (10, 30, 100, 300, 1,000, 3,000, and 7,000 μM) and the amounts of *CLE* gene transcripts were quantified by real-time PCR. Results are given in relative transcript abundance relative to the sample from 7,000 μM NO_3^-. Ubiquitin 2 was used as an internal standard. Error bars denote SEM ($n = 5$). Significant differences obtained by Tukey's multiple test at $P < 0.05$ are shown by different letters. (*B–D*) Root phenotypes of wild-type (Col-0) and *CLE2* and *CLE3* overexpressor lines. The primary root length (*C*) and the total length of visible lateral roots (*D*) were measured in 11-d-old plants grown vertically on medium containing 100 μM NO_3^-. Error bars denote SEM ($n = 13–21$). Graphs separated by a vertical bar indicate results from independent experiments. (*E*) Lateral root (LR) density of wild-type (Col-0) and *CLE2* and *CLE3* overexpressor lines classified by developmental stages. Plants were grown vertically on medium containing 100 μM NO_3^- for 7 d. Error bars denote SEM ($n = 27–36$). Significant differences with Dunnett's multiple test at $*P < 0.05$ or $**P < 0.01$ are shown. (*F*) Relative frequency distribution of lateral root primordia and lateral roots. The relative frequency of lateral root primordia or lateral roots in each developmental stage is indicated by their percentage in the total number of lateral root initiation events. The size of each circle indicates the total lateral root density shown in *E*. (*G* and *H*) GFP expression in *CLE3* promoter:GFP plants. Plants were grown vertically on medium containing 10 μM NO_3^- for 7 d. Longitudinal (*G*) and cross (*H*) sections of primary roots indicate specific localization of GFP signals (green) in the pericycle (p). Roots for cross sections were counter stained by propidium iodide (red). c, cortex; en, endodermis; ep, epidermis; p, pericycle. [Scale bars, 100 μm (*G*) and 50 μm (*H*).]

the *CLE* overexpressors than in the wild-type (Fig. 1 *B–D* and Fig. S1 *H–J*). The effect of *CLE* transgenes on lateral root growth inhibition was more significant under conditions of moderate to high nitrate supply (Fig. S1*L*), where endogenous *CLEs* were repressed (Fig. 1*A*).

We further conducted microscopic analysis to determine the number of lateral root primordia and emerged lateral roots (Fig. 1 *E* and *F*, and Fig. S2 *B* and *C*). For this purpose, the total number of lateral root-initiation events was counted, and lateral root primordia and emerged lateral roots were classified according to the developmental stages I–IV, V–VII, and VIII (42). Although the total lateral root density (the sum of unemerged lateral root primordia and emerged lateral roots) was not different between the overexpressors and the wild-type, the density of emerged lateral roots at stage VIII was dramatically decreased by overexpression of *CLE1*, *-2*, *-3*, *-4*, and *-7* (Fig. 1*E* and Fig. S2*B*). This finding was also evident from a decreased frequency of emerged lateral roots (stage VIII) and a proportionally increased frequency of unemerged lateral root primordia at stages I–IV in the overexpressors relative to the wild-type (Fig. 1*F* and Fig. S2*C*). These results indicated that overexpression of *CLE1*, *-2*, *-3*, *-4*, and *-7* can repress the outgrowth of lateral root primordia and their emergence from the primary root but do not affect lateral root initiation. In promoter:GFP lines, *CLE1*, *-2*, *-3*, *-4*, and *-7* promoter activities were predominantly localized in pericycle cells of primary and lateral roots (Fig. 1 *G* and *H* and Fig. S2*D*), similar to the results shown by promoter:GUS analyses (43). In *CLE1* and *-5* promoter:GFP lines, GFP was expressed

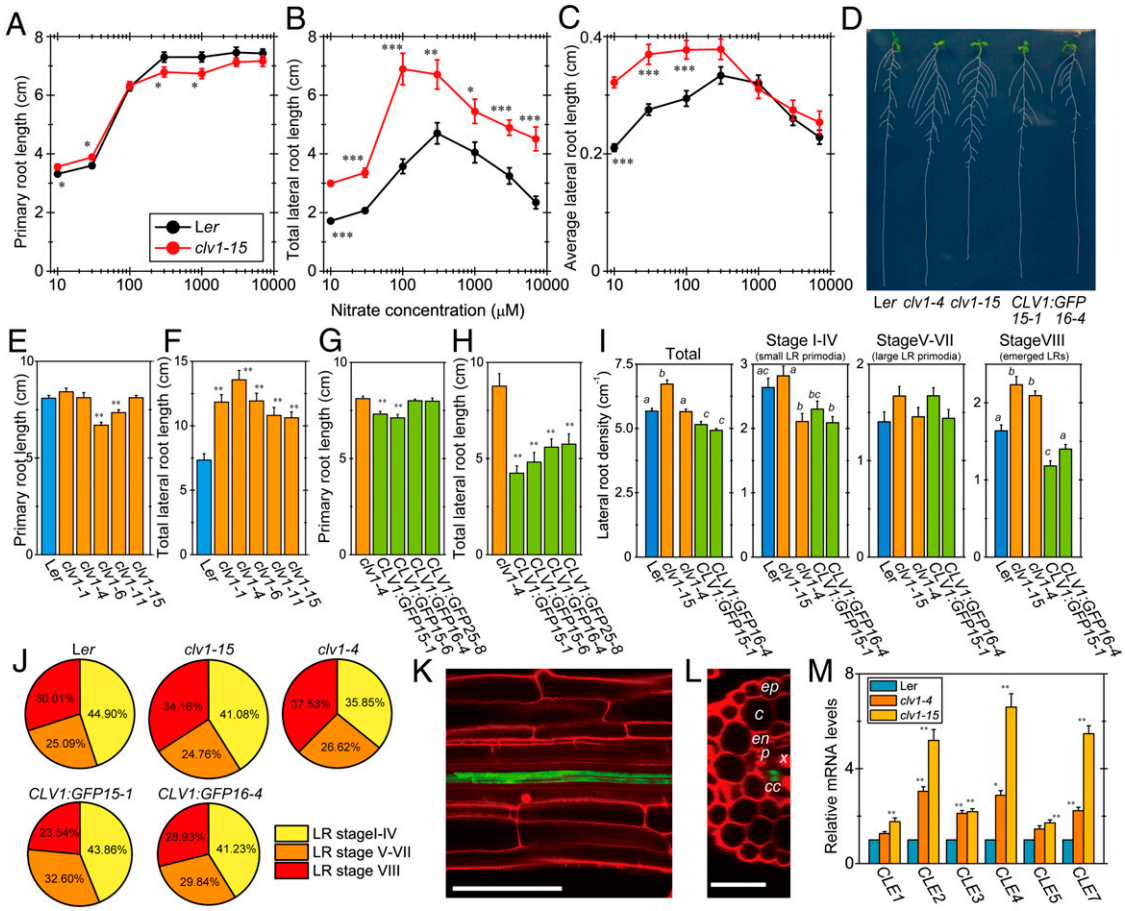

Fig. 2. Regulation of lateral root development by CLV1. (*A–C*) Effect of N deficiency on root traits of wild-type (L*er*) and *clv1-15* mutant plants. Plants were grown vertically for 11 d on medium with various NO_3^- concentrations (10, 30, 100, 300, 1,000, 3,000, and 7,000 μM). Primary root length (*A*), total lateral root length (*B*), and average lateral root length (*C*) were quantified as in Fig. 1. Error bars denote SEM (n = 26–51). Average lateral root length (*C*) was calculated by dividing the total lateral root length by the number of visible lateral roots. Significant differences between L*er* and *clv1-15* at each NO_3^- concentration are shown as $*P < 0.05$, $**P < 0.01$, or $***P < 0.001$ according to Student t tests. (*D*) Root phenotypes of wild-type (L*er*), *clv1* mutants, and CLV1:GFP plants. Plants were grown vertically on medium containing 100 μM NO_3^- for 11 d. The roots are traced by a white line to increase the contrast. The original image without tracing is shown in Fig. S4*B*. (*E* and *F*) Root length comparison between wild type (L*er*) and *clv1* mutants. Error bars denote SEM (n = 20–29). Plants were grown as shown in *D*. Asterisks (**) indicate statistically significant differences from L*er* with Dunnett's multiple test ($P < 0.01$). (*G and H*) Root phenotypes of *CLV1:GFP* lines in the *clv1-4* background. Error bars denote SEM (n = 24–28). Plants were grown as shown in *D*. Asterisks (**) indicate statistically significant differences from *clv1-4* with Dunnett's multiple test ($P < 0.001$). (*I*) Lateral root (LR) densities of *clv1* mutants and *CLV1:GFP* lines in *clv1-4* background classified by developmental stages. Plants were grown vertically on medium containing 100 μM NO_3^- for 7 d. Error bars denote SEM (n = 39–42). Significant differences at $P < 0.05$ with Tukey's multiple test are indicated by different letters. (*J*) Relative frequency distribution of lateral root primordia and lateral roots. The relative frequency of lateral root primordia or lateral roots in each developmental stage is indicated by their percentage in the total number of lateral root initiation events. The size of each circle indicates the total lateral root density shown in *I*. *(K and L)* Localization of CLV1:GFP in roots. Green signals in longitudinal (*K*) and cross (*L*) sections of a primary root indicate localization of CLV:GFP fusion proteins in phloem companion cells (cc). The root was counter-stained with propidium iodide (red). c, cortex; cc, companion cell; en, endodermis; ep, epidermis; p, pericycle; x, xylem. [Scale bars, 100 μm (*K*) and 50 μm (*L*).] (*M*) *CLE1* to seven transcripts overaccumulate in *clv1* mutants. Results are shown as transcript abundance in *clv1* mutants relative to the wild-type (L*er*). Error bars denote SEM (n = 4). Significant differences with Dunnett's multiple test at $*P < 0.05$ or $**P < 0.01$ are shown.

in epidermal cells of the primary root tip (Fig. S2*D*). These partly overlapping spatial expression patterns suggested a functional redundancy among *CLE1*, *-2*, *-3*, *-4*, and *-7*, consistent with our finding that overexpression of any of the corresponding genes is sufficient to inhibit lateral root development (Fig. 1 *B–F*, Fig. S1 *H–J*, and Fig. S2 *B* and *C*).

CLV1 Regulates Lateral Root Development. The peptide sequences of the N-responsive CLE homologs CLE1 to -7 are highly homologous to CLV3 (21–23), which binds to the receptor CLV1 (25–32). To investigate the signaling pathways associated with CLE1 to -7 in roots, the knockout mutants of type XI LRR-RLKs including phylogenetically close members of CLV1 were collected (44), and their root phenotypes were examined under low N conditions. Among these mutants, only *clv1* showed a significant extension of lateral roots (Fig. S3*A*), which was opposite to the short lateral root phenotypes observed in *CLE1* to *-7* overexpressors (Fig. 1). We further investigated the root developmental traits of *Arabidopsis* seedlings under various N conditions, using the *clv1-15* mutant obtained from the Ds transposon-inserted line collection (45) and L*er* as the wild-type (Fig. 2 *A–C*). The wild-type seedlings (L*er*) showed a significant decrease in total or average lateral root length under severe N deficiency (i.e., below 100 μM NO_3^-) (Fig. 2 *B* and *C*). In contrast, when *clv1-15* was grown under the same condition, total and average lengths of lateral roots were significantly longer than those in the wild-type (Fig. 2 *B* and *C*). The primary roots of the wild-type and *clv1-15* showed similar lengths and trends to decrease under N deficiency (Fig. 2*A*). From these results, CLV1 was suggested to mediate the N-responsive CLE peptide signaling pathways controlling lateral root development under N-deficient conditions.

A repressive action of CLV1 on lateral root development was further supported by the analysis of root traits in allelic mutants of *clv1* (46, 47) and in transgenic lines expressing the *CLV1* promoter-driven *CLV1:GFP* fusion gene (Fig. S4*A*) in the *clv1-4* background. On low-N medium, five allelic mutants of *clv1* (*clv1-1*, *clv1-4*, *clv1-6*, *clv1-11*, and *clv1-15*) exhibited significantly elongated lateral roots compared with the wild-type (Fig. 2 *D* and *F*), whereas expression of *CLV1:GFP* in *clv1-4* reverted these root phenotypes (Fig. 2 *D* and *H*). These results indicated that the CLV1:GFP fusion protein was capable of restoring the root phenotypes in *clv1-4*. Although lateral root length was significantly altered, primary root length was not consistently affected in *clv1* mutants or *CLV1:GFP* lines (Fig. 2 *E* and *G*).

Microscopic analysis indicated that the density of emerged lateral roots (stage VIII) was significantly increased in *clv1* mutants relative to wild-type plants (Fig. 2*I*). This result was expressed by an increased frequency of emerged lateral roots (stage VIII) and a proportional decrease in unemerged lateral root primordia at stages I–IV (Fig. 2*J*). Subsequent analysis of two *CLV1:GFP* lines (*CLV1:GFP 15-1* and *16-4*) with their background line (*clv1-4*) showed that the density of emerged lateral roots was substantially decreased by expression of *CLV1:GFP* (Fig. 2*I*). This result was also shown by a decreased frequency of these emerged lateral roots and an increased frequency of unemerged lateral root primordia at stages I–IV in the *CLV1:GFP* lines relative to the *clv1-4* mutant (Fig. 2*J*). Total lateral root densities were slightly increased in *clv1-15* and decreased in *CLV1:GFP* lines; however, these changes were mostly projected on the number of emerged lateral roots indicating the effect on stage progression (Fig. 2 *I* and *J*). Taken together, this set of experiments indicated a repressive role of CLV1 in regulating the growth of lateral root primordia and their emergence from the primary root.

Confocal microscopy revealed localization of CLV1:GFP fusion proteins in the phloem companion cells of both primary and lateral roots (Fig. 2 *K* and *L* and Fig. S4*C*), indicating their spatial separation from pericycle cells where *CLE1*, *-2*, *-3*, *-4*, and *-7* promoter activities were predominantly localized (Fig. 1 *G* and *H* and Fig. S2*D*). In shoots, CLV1:GFP was found in the shoot apical meristem (Fig. S4*D*) and restored the silique-defective phenotype of *clv1-4* (Fig. S4*E*), indicating its ability to fulfill a similar function as the CLV1:double-GFP fusion protein (32). Thus, CLV1 and CLE1 to -7 were localized in different cell types in roots, although they both conferred an inhibition of lateral root development under N-deficient conditions (Figs. 1 and 2). To further investigate their relationship in roots, we analyzed *CLE1* to *-7* transcript levels in wild-type and *clv1* roots and observed a significant overaccumulation of *CLE2*, *-3*, *-4*, and *-7* in *clv1-4* and *clv1-15* (Fig. 2*M*). *CLE1* and *CLE5* mRNA levels accumulated to a lower extent in *clv1*. These results suggested feedback regulation of *CLE2*, *-3*, *-4*, and *-7* by CLV1 in wild-type roots, as observed for *CLV3* in the shoot apical meristem (27, 28).

CLE3-Induced Inhibition of Lateral Root Development Requires CLV1. Based on results obtained from analysis of *CLE* overexpressors and *clv1* mutants, we hypothesized that overexpression of N-responsive induction of *CLEs* in roots should cause inhibition of lateral root development in wild-type but not in *clv1* mutant plants, if the CLE-CLV1 signaling module is functional in roots. To test this hypothesis, transgenic lines were prepared to overexpress *CLE3* under control of its native promoter in the wild-type and *clv1-4* mutant background (Fig. 3 and Fig. S5). *CLE3* was chosen for this experiment because it was among the most up-regulated *CLE* genes under N deficiency (Fig. 1). To enhance transcriptional/translational efficiency yet conserving the original expression pattern of *CLE3* in roots, we inserted a cauliflower mosaic virus 35S gene minimal promoter (35Smin) (48) and a tobacco mosaic virus-derived Ω sequence (49) between the native *CLE3* promoter and the coding region (Fig. S5*A*). The resulting CLE3 promoter-35Smin-Ω-CLE3 (C3P3) fusion construct was introduced into wild-type (L*er*) and *clv1-4* mutant plants and root phenotypes were analyzed. In *CLE3* promoter-35Smin-Ω-GFP (C3PG) lines, a strong promoter activity was found in the central cylinder of roots and in primary and lateral root tips (Fig. S5 *B* and *C*). Unlike transgenic lines that constitutively expressed *CLE1* to *-7* (Fig. S2*A*), C3P3-expressing lines in wild-type (L*er*) background did not show any phenotypic defects in shoots and the shoot apical meristem (Fig. S5*D*).

C3P3-expressing lines were then subjected to a quantitative assessment of lateral root phenotypes (Fig. 3 *A* and *B*). Root lengths and *CLE3* mRNA levels were examined in 80 individual seedlings from the T2 generation by collecting 10–14 individuals from seven independent transgenic lines each from the L*er* or *clv1-4* background. Root lengths of individual seedlings were normalized by values of their backgrounds (L*er* or *clv1-4*) to compare the relative effect of *CLE3* overexpression in these two different populations (absolute values are shown in Fig. S5 *E* and *F*). These normalized root-length values (PR_{sample}/PR_{cont} or LR_{sample}/LR_{cont}) were then plotted against *CLE3* mRNA levels (Fig. 3 *A* and *B*). The slope of the regression line indicates the quantitative extent of root growth inhibition caused by increasing *CLE3* expression levels. The results indicated that primary root length was not altered by *CLE3* expression in either background (Fig. 3*A*). In contrast, total lateral root length was substantially decreased with increasing *CLE3* expression levels in L*er* but only slightly in *clv1-4* (Fig. 3*B*). As revealed by the top three lines showing the highest *CLE3* mRNA levels in either background (Fig. S5 *G* and *H*), root-specific expression of *CLE3* inhibited lateral root development in wild-type but not in *clv1-4* mutant plants. The slope of the regression line was −0.34 for the L*er* but only −0.09 for the *clv1-4* background, demonstrating that an almost fourfold greater reduction of total lateral root length occurred in wild-type relative to *clv1-4* mutant plants (Fig. 3*B*). The significant difference in CLE3-dependent inhibition of lateral root development between L*er* and *clv1-4* was supported by an analysis of covariance ($P < 0.001$).

Discussion

This study demonstrates that the CLE-CLV1 signaling pathway is a core module for regulating the expansion of the lateral root system in *Arabidopsis* in low N environments. The results

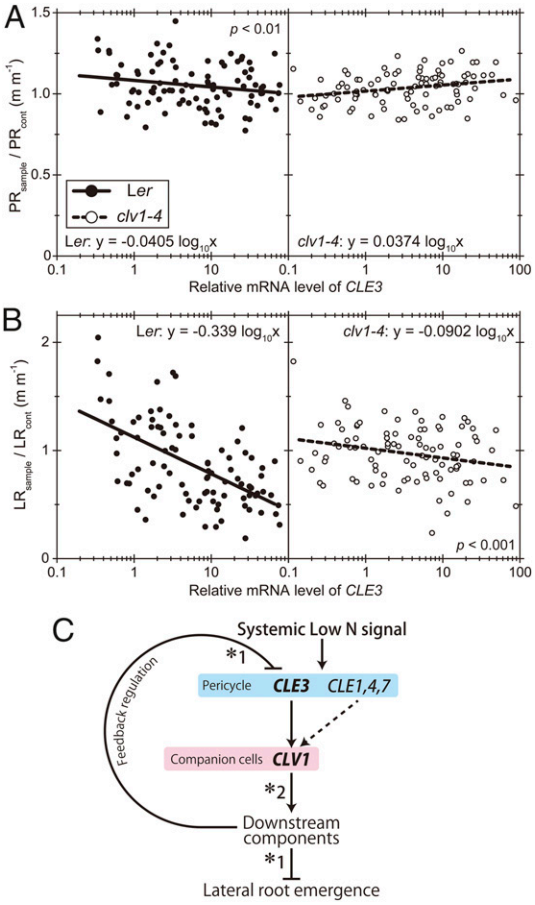

Fig. 3. Effect of CLE3 in wild-type and *clv1* mutant plants. (*A* and *B*) Correlation between root length and *CLE3* mRNA levels in C3P3-expressing L*er* or *clv1-4* plants. Primary root (PR) length (*A*) and total lateral root (LR) length (*B*) of individual seedlings are given relative to the respective background line. Relative root length values were calculated by normalizing the values of individual samples (PR_{sample} or LR_{sample}) with those of the background lines (i.e., L*er* or *clv1-4*) (PR_{cont} or LR_{cont}) ($n = 14$). L*er* plants were used as standard samples for relative quantification of *CLE3* mRNA levels by real-time RT-PCR. Closed and open symbols correspond to individual lines in L*er* and *clv1-4* backgrounds. A linear regression was calculated for the L*er* (solid line) and *clv1-4* background (dotted line). Plants were grown vertically on medium containing 100 μM NO_3^- for 11 d. The differences between the slopes in L*er* and *clv1-4* backgrounds are shown by *P* values of analysis of covariance. The details of the regression analysis and statistical values are summarized in Table S1. (*C*) Model for the regulation of lateral root development by the CLE-CLV1 signaling module. The N deficiency and the feedback mechanism counteractively modulate the amplitude of the CLE signals repressing the growth of lateral root primordia and their emergence from the primary root. Inhibitory signals (*1) and a positive signal (*2) can be opposite such that CLV1 represses a downstream positive factor.

presented here indicate that the outgrowth and emergence of lateral root primordia rather than their initiation accounted for this morphological response (Figs. 1 and 2). The morphological response governed by the CLE-CLV1 pathway is thus suggested to be distinct from lateral root initiation mechanisms known to be stimulated under N supply (9, 14–16) or controlled by NRT2.1 (12, 19). The low-N responsive induction of *CLE1*, *-3*, *-4*, and *-7* as well as the phenotypes of *CLE* overexpressors and *clv1* mutants provided evidence that CLE peptides and CLV1 are components of regulatory mechanisms controlling the same root developmental trait associated with growth of lateral root primordia under N-deficient conditions (Figs. 1 and 2). Moreover, the inhibitory effect of CLE3 on lateral root development was shown to be dependent on CLV1 (Fig. 3*B*). These key observations led us to propose a model that highlights a predominant role of CLV1 in mediating CLE-derived signals for repressing lateral root development under N deficiency (Fig. 3*C*). The mRNA overaccumulation of *CLE2*, *-3*, *-4*, and *-7* in *clv1* mutants (Fig. 2*M*) further supports this relationship with CLV1 being placed in a regulatory circuit where a feedback loop controls the amplitude of the CLE peptide signals (Fig. 3*C*).

The cell type-specific localization of GFP fusion proteins indicated that CLV1 is expressed in phloem companion cells (Fig. 2 *K* and *L* and Fig. S4*C*), whereas *CLE1*, *-2*, *-3*, *-4*, and *-7* were expressed in the pericycle (Fig. 1 *G* and *H*, and Fig. S2*D*). Based on these specific patterns of gene expression, CLE peptides are hypothesized to be secreted from pericycle cells and transported through the apoplastic continuum within the central cylinder to reach companion cells where CLV1 resides at the plasma membrane (Fig. 3*C*). The information on the N nutritional status would integrate in pericycle cells to modulate the expression levels of these *CLE* mRNAs. CLE peptides are suggested to carry the information from pericycle to phloem companion cells where the CLE-CLV1 module further elicits downstream signals inhibiting the growth of lateral root primordia. The feedback regulation of *CLE* transcript accumulation by CLV1 (Fig. 2*M*) suggests that a phloem-derived signal downstream of CLV1 may also integrate into this regulatory mechanism to modulate the strength of the signal (Fig. 3*C*). In this model, CLV1 remains at a central checkpoint for modulating the strength of N-dependent signals controlling the growth and emergence of lateral root primordia, whereas CLE peptides (CLE1, -3, -4, and -7) regulated at the transcript level may be seen as a quantitative readout of the N status. *CLE1* and *CLE5* expression also occurred in root tips (Fig. S4), suggesting that their corresponding peptides may have additional functions.

Our results further indicate that lateral root development is inhibited by *CLE3* expression levels in a dose-dependent manner (Fig. 3*B*), suggesting that the strength of the CLE signal is directly translated into a morphological response. The action of the CLE3 signal was abrogated in the *clv1-4* mutant, emphasizing the role of CLV1 as the major receptor of CLE3-dependent signaling for this root trait and as a determinant affecting lateral root morphology. However, because the inhibitory effect of CLE3 was not completely abolished in the *clv1-4* mutant background, other colocalized LRR-RLK proteins may have bound CLE3 or other CLE peptides to provoke similar but marginal functions in lateral root development.

The induction of *CLE3* gene expression triggers the inhibition of the outgrowth of lateral root primordia and their emergence from the primary root (Fig. 3*C*). We assume that CLE1, -3, -4, and -7 redundantly and cumulatively act on the CLE-CLV1 signaling pathway by sharing CLV1 as a common receptor. Because this signaling module takes action under prolonged N deficiency, it serves as a mechanism to prevent the expansion of the lateral root system into N-poor environments (4). This study emphasizes the importance of intercellular signaling mechanisms in the root vasculature translating N nutritional information into root morphological responses.

Materials and Methods

Plant Growth. For root phenotypic analysis, *Arabidopsis* plants were grown vertically on nutrient media (50) containing 1% agar and 1% sucrose under a diurnal cycle of 16-h light and 8-h dark at 22 °C. To modify NO_3^- concentrations in the medium, $Ca(NO_3)_2$ or KNO_3 were replaced with $CaCl_2$ or KCl, respectively. The *clv1-1*, *clv1-4*, *clv1-6*, and *clv1-11* are L*er* background mutants reported previously (46, 47). The *clv1-15* mutant (ET13689) was obtained from the Ds transposon-inserted line collection (45). The LRR-RLK type XI knockout mutants (44) are in Col background. Transgenic *Arabidopsis* plants were constructed as described in *SI Materials and Methods*.

Root Phenotypic Analysis. Plants grown on vertical plates were scanned (EPSON Perfection 4990 PHOTO; Seiko Epson), and the images of roots were traced using Photoshop CS2 (Adobe Systems). Root lengths were measured from traced images using WinRHIZO (Reagent Instruments). For the determination of lateral root numbers, plants were grown on agar medium for 7 d, and roots were cleared with hydroxylamine hydrochloride (42).

Lateral root number was counted under a microscope, and lateral root initials and emerged lateral roots were classified to stages I–IV, V–VII, and VIII (42) for separate calculation of their densities (i.e., numbers of lateral root primordia or lateral roots per unit length of primary root). The primary root length was measured from the scanned images using WinRHIZO, as described above.

Quantitative Real-Time PCR. Total RNA was extracted from roots using RNeasy plant mini kit (Qiagen). First-strand cDNA was synthesized from 500 ng of total RNA using omniscript reverse transcriptase (Qiagen) and oligo-d(T)$_{12-18}$ primer (Invitrogen), and was used for quantitative real-time PCR. Real-time RT-PCR was performed by using SYBR Premix Ex Taq II (Takara) and 7500 Fast Real-Time PCR system (Applied Biosystems). Relative transcript levels were calculated by comparative cycle threshold method (ΔΔCt method). Ubiquitin 2 was used as an internal control. The primer sequences for real-time PCR are listed in Table S2.

Imaging of GFP Expression. Expression of GFP was analyzed with the laser scanning confocal microscopy system FluoView 500 (Olympus). Roots of *CLE3* promoter:GFP, *CLV1:GFP* and *C3PG* plants were counter stained with propidium iodide.

ACKNOWLEDGMENTS. We thank K. Nojima, M. Funatsu, Y. Suzuki, and C. Komori for technical support. This work was supported in part by the Bio-oriented Technology Research Advancement Institution (BRAIN) of Japan and by the Deutsche Forschungsgemeinschaft (WI1728/13-1).

1. López-Bucio J, Cruz-Ramírez A, Herrera-Estrella L (2003) The role of nutrient availability in regulating root architecture. *Curr Opin Plant Biol* 6(3):280–287.
2. Hodge A (2004) The plastic plant: Root responses to heterogeneous supplies of nutrients. *New Phytol* 162(1):9–24.
3. Robinson D (1994) The responses of plants to non-uniform supplies of nutrients. *New Phytol* 127(4):635–674.
4. Gruber BD, Giehl RFH, Friedel S, von Wirén N (2013) Plasticity of the *Arabidopsis* root system under nutrient deficiencies. *Plant Physiol* 163(1):161–179.
5. Drew MC (1975) Comparison of the effects of a localised supply of phosphate, nitrate, ammonium and potassium on the growth of the seminal root system, and the shoot, in barley. *New Phytol* 75(3):479–490.
6. Robinson D, Hodge A, Griffiths BS, Fitter AH (1999) Plant root proliferation in nitrogen-rich patches confers competitive advantage. *Proc R Soc Lond B* 266(1418):431–435.
7. Zhang H, Forde BG (1998) An *Arabidopsis* MADS box gene that controls nutrient-induced changes in root architecture. *Science* 279(5349):407–409.
8. Remans T, et al. (2006) The *Arabidopsis* NRT1.1 transporter participates in the signaling pathway triggering root colonization of nitrate-rich patches. *Proc Natl Acad Sci USA* 103(50):19206–19211.
9. Lima JE, Kojima S, Takahashi H, von Wirén N (2010) Ammonium triggers lateral root branching in *Arabidopsis* in an AMMONIUM TRANSPORTER1;3-dependent manner. *Plant Cell* 22(11):3621–3633.
10. Zhang H, Jennings A, Barlow PW, Forde BG (1999) Dual pathways for regulation of root branching by nitrate. *Proc Natl Acad Sci USA* 96(11):6529–6534.
11. Forde B, Lorenzo H (2001) The nutritional control of root development. *Plant Soil* 232(1):51–68.
12. Remans T, et al. (2006) A central role for the nitrate transporter NRT2.1 in the integrated morphological and physiological responses of the root system to nitrogen limitation in *Arabidopsis*. *Plant Physiol* 140(3):909–921.
13. Ruffel S, et al. (2011) Nitrogen economics of root foraging: Transitive closure of the nitrate-cytokinin relay and distinct systemic signaling for N supply vs. demand. *Proc Natl Acad Sci USA* 108(45):18524–18529.
14. Gifford ML, Dean A, Gutierrez RA, Coruzzi GM, Birnbaum KD (2008) Cell-specific nitrogen responses mediate developmental plasticity. *Proc Natl Acad Sci USA* 105(2):803–808.
15. Vidal EA, et al. (2010) Nitrate-responsive *miR393/AFB3* regulatory module controls root system architecture in *Arabidopsis thaliana*. *Proc Natl Acad Sci USA* 107(9):4477–4482.
16. Vidal EA, Moyano TC, Riveras E, Contreras-López O, Gutiérrez RA (2013) Systems approaches map regulatory networks downstream of the auxin receptor AFB3 in the nitrate response of *Arabidopsis thaliana* roots. *Proc Natl Acad Sci USA* 110(31):12840–12845.
17. Krouk G, et al. (2010) Nitrate-regulated auxin transport by NRT1.1 defines a mechanism for nutrient sensing in plants. *Dev Cell* 18(6):927–937.
18. Ho C-H, Lin S-H, Hu H-C, Tsay Y-F (2009) CHL1 functions as a nitrate sensor in plants. *Cell* 138(6):1184–1194.
19. Little DY, et al. (2005) The putative high-affinity nitrate transporter NRT2.1 represses lateral root initiation in response to nutritional cues. *Proc Natl Acad Sci USA* 102(38):13693–13698.
20. Cock JM, McCormick S (2001) A large family of genes that share homology with CLAVATA3. *Plant Physiol* 126(3):939–942.
21. Ito Y, et al. (2006) Dodeca-CLE peptides as suppressors of plant stem cell differentiation. *Science* 313(5788):842–845.
22. Mitchum MG, Wang X, Davis EL (2008) Diverse and conserved roles of CLE peptides. *Curr Opin Plant Biol* 11(1):75–81.
23. Oelkers K, et al. (2008) Bioinformatic analysis of the CLE signaling peptide family. *BMC Plant Biol* 8:1.
24. Betsuyaku S, Sawa S, Yamada M (2011) The function of the CLE peptides in plant development and plant-microbe interactions. *Arabidopsis Book* 9:e0149.
25. Clark SE, Williams RW, Meyerowitz EM (1997) The *CLAVATA1* gene encodes a putative receptor kinase that controls shoot and floral meristem size in *Arabidopsis*. *Cell* 89(4):575–585.
26. Fletcher JC, Brand U, Running MP, Simon R, Meyerowitz EM (1999) Signaling of cell fate decisions by *CLAVATA3* in *Arabidopsis* shoot meristems. *Science* 283(5409):1911–1914.
27. Brand U, Fletcher JC, Hobe M, Meyerowitz EM, Simon R (2000) Dependence of stem cell fate in *Arabidopsis* on a feedback loop regulated by *CLV3* activity. *Science* 289(5479):617–619.
28. Schoof H, et al. (2000) The stem cell population of *Arabidopsis* shoot meristems in maintained by a regulatory loop between the *CLAVATA* and *WUSCHEL* genes. *Cell* 100(6):635–644.
29. Kondo T, et al. (2006) A plant peptide encoded by *CLV3* identified by in situ MALDI-TOF MS analysis. *Science* 313(5788):845–848.
30. Ogawa M, Shinohara H, Sakagami Y, Matsubayashi Y (2008) *Arabidopsis* CLV3 peptide directly binds CLV1 ectodomain. *Science* 319(5861):294.
31. Ohyama K, Shinohara H, Ogawa-Ohnishi M, Matsubayashi Y (2009) A glycopeptide regulating stem cell fate in *Arabidopsis thaliana*. *Nat Chem Biol* 5(8):578–580.
32. Nimchuk ZL, Tarr PT, Ohno C, Qu X, Meyerowitz EM (2011) Plant stem cell signaling involves ligand-dependent trafficking of the CLAVATA1 receptor kinase. *Curr Biol* 21(5):345–352.
33. De Smet I, et al. (2008) Receptor-like kinase ACR4 restricts formative cell divisions in the *Arabidopsis* root. *Science* 322(5901):594–597.
34. Stahl Y, Wink RH, Ingram GC, Simon R (2009) A signaling module controlling the stem cell niche in *Arabidopsis* root meristems. *Curr Biol* 19(11):909–914.
35. Stahl Y, et al. (2013) Moderation of *Arabidopsis* root stemness by CLAVATA1 and ARABIDOPSIS CRINKLY4 receptor kinase complexes. *Curr Biol* 23(5):362–371.
36. Strabala TJ, et al. (2006) Gain-of-function phenotypes of many *CLAVATA3/ESR* genes, including four new family members, correlate with tandem variations in the conserved *CLAVATA3/ESR* domain. *Plant Physiol* 140(4):1331–1344.
37. Ni J, Clark SE (2006) Evidence for functional conservation, sufficiency, and proteolytic processing of the CLAVATA3 CLE domain. *Plant Physiol* 140(2):726–733.
38. Scheible W-R, et al. (2004) Genome-wide reprogramming of primary and secondary metabolism, protein synthesis, cellular growth processes, and the regulatory infrastructure of *Arabidopsis* in response to nitrogen. *Plant Physiol* 136(1):2483–2499.
39. Patterson K, et al. (2010) Distinct signalling pathways and transcriptome response signatures differentiate ammonium- and nitrate-supplied plants. *Plant Cell Environ* 33(9):1486–1501.
40. Wang R, Okamoto M, Xing X, Crawford NM (2003) Microarray analysis of the nitrate response in *Arabidopsis* roots and shoots reveals over 1,000 rapidly responding genes and new linkages to glucose, trehalose-6-phosphate, iron, and sulfate metabolism. *Plant Physiol* 132(2):556–567.
41. Wang R, et al. (2004) Genomic analysis of the nitrate response using a nitrate reductase-null mutant of *Arabidopsis*. *Plant Physiol* 136(1):2512–2522.
42. Malamy JE, Benfey PN (1997) Organization and cell differentiation in lateral roots of *Arabidopsis thaliana*. *Development* 124(1):33–44.
43. Jun J, et al. (2010) Comprehensive analysis of *CLE* polypeptide signaling gene expression and overexpression activity in *Arabidopsis*. *Plant Physiol* 154(4):1721–1736.
44. Hirakawa Y, et al. (2008) Non-cell-autonomous control of vascular stem cell fate by a CLE peptide/receptor system. *Proc Natl Acad Sci USA* 105(39):15208–15213.
45. Sundaresan V, et al. (1995) Patterns of gene action in plant development revealed by enhancer trap and gene trap transposable elements. *Genes Dev* 9(14):1797–1810.
46. Clark SE, Running MP, Meyerowitz EM (1993) *CLAVATA1*, a regulator of meristem and flower development in *Arabidopsis*. *Development* 119(2):397–418.
47. Diévart A, et al. (2003) CLAVATA1 dominant-negative alleles reveal functional overlap between multiple receptor kinases that regulate meristem and organ development. *Plant Cell* 15(5):1198–1211.
48. Odell JT, Nagy F, Chua NH (1985) Identification of DNA sequences required for activity of the cauliflower mosaic virus 35S promoter. *Nature* 313(6005):810–812.
49. Mitsuhara I, et al. (1996) Efficient promoter cassettes for enhanced expression of foreign genes in dicotyledonous and monocotyledonous plants. *Plant Cell Physiol* 37(1):49–59.
50. Fujiwara T, Hirai MY, Chino M, Komeda Y, Naito S (1992) Effects of sulfur nutrition on expression of the soybean seed storage protein genes in transgenic petunia. *Plant Physiol* 99(1):263–268.